Articles

Structure of the Smooth Muscle Myosin Light-Chain Kinase Calmodulin-Binding Domain Peptide Bound to Calmodulin†

Sharon M. Roth,‡,§ Diane M. Schneider,‡,§ Laura A. Strobel,‡ Mark F. A. VanBerkum,∥,⊥ Anthony R. Means,∥,○ and A. Joshua Wand*,‡,§,#

Institute for Cancer Research, Fox Chase Cancer Center, 7701 Burholme Avenue, Philadelphia, Pennsylvania, 19111, Department of Biochemistry, University of Illinois at Urbana-Champaign, Urbana, Illinois 61801, and Department of Cell Biology, Baylor College of Medicine, Houston, Texas 77030

Received July 15, 1991; Revised Manuscript Received August 22, 1991

ABSTRACT: The interaction between the peptide corresponding to the calmodulin-binding domain of the smooth muscle myosin light-chain kinase and $(Ca^{2+})_4$-calmodulin has been studied by multinuclear and multidimensional nuclear magnetic resonance methods. The study was facilitated by the use of ^{15}N-labeled peptide in conjunction with ^{15}N-edited and ^{15}N-correlated ^1H spectroscopy. The peptide forms a 1:1 complex with calcium-saturated calmodulin which is in slow exchange with free peptide. The ^1H and ^{15}N resonances of the bound have been assigned. An extensive set of structural constraints for the bound peptide has been assembled from the analysis of nuclear Overhauser effects and three-bond coupling constants. The backbone conformation of the bound peptide has been determined using these constraints by use of distance geometry and related computational methods. The backbone conformation of the peptide has been determined to high precision and is generally indicative of helical secondary structure. Nonhelical backbone conformations are seen in the middle and at the C-terminal end of the bound peptide. These studies provide the first direct confirmation of the amphiphilic helix model for the structure of peptides bound to calcium-saturated calmodulin.

The means by which calmodulin regulates a large variety of enzymes involved in a diverse collection of cellular processes has been the subject of intense investigation. The mediation by calmodulin of cellular responses to changes in calcium concentration is an intriguing example of the coupling of extracellular messengers to fundamental biological responses. An understanding of the molecular basis of the transduction of changes in Ca^{2+} levels to changes in target enzyme activity is only now beginning to emerge. Calmodulin is a small acidic protein capable of binding four Ca^{2+} ions. Both the solution (Ikura et al., 1990) and crystal (Babu et al., 1985, 1989) structures of calcium-saturated calmodulin (CaM)[1] have two globular domains, each containing two helix–loop–helix motifs. A most striking feature of the crystal is a long α helix joining the two globular domains.

Over the past few years a number of naturally occurring peptides, such as the bee and wasp venom peptides, have been found to bind to calmodulin in a Ca^{2+}-dependent manner with very high affinity ($K_d \leq 1$ nM) (Comte et al., 1983; McDowell et al., 1985). More recently, the calmodulin-binding domains of a number of calmodulin-regulated enzymes have been defined by use of synthetic peptide analogues [e.g., Blumenthal et al. (1985), Kemp et al. (1987), Dasgupta et al. (1989), and Vorherr et al. (1990)]. These and other studies [e.g., McDowell et al. (1985), Cox et al. (1985), O'Neil et al. (1987), and O'Neil and DeGrado (1990)] have led to the conclusion that basic, amphiphilic peptides capable of forming high-affinity complexes in a calcium-dependent manner do so by adopting a helical conformation in the bound state.

The connection between the amphiphilic helical model for the structures of the bound peptide and the structure(s) of calmodulin–peptide complexes has been made in several model-building studies [e.g., O'Neil and DeGrado (1985), Persechini and Krestinger (1988), and Strynadka and James (1990)]. All of these studies rest, to varying degrees, on significant assumptions regarding the structures of the individual components. In this regard, considerable evidence has recently been presented to indicate that the backbone structure of the globular domains of calmodulin is not greatly perturbed when bound to synthetic peptides corresponding to the cal-

† This work was supported by NIH Research Grants DK-39806 (A. J.W.) and GM-33926 (A.R.M.), by NIH grants CA-06927 and RR-05539, by an appropriation from the Commonwealth of Pennsylvania, and by a grant from the Fanny Ripple Foundation awarded to the Institute for Cancer Research. D.M.S. is the recipient of an NIH postdoctoral fellowship (GM-12594). S.M.R. is the recipient of an NIH predoctoral fellowship administered by the University of Pennsylvania (GM-07229).

* Address correspondence to this author at the University of Illinois.
‡ Fox Chase Cancer Center.
§ University of Illinois.
∥ Baylor College of Medicine.
⊥ Present address: Department of Molecular and Cellular Biology, University of California, Berkeley, CA 94720.
○ Present address: Department of Pharmacology, Duke University Medical Center, Durham, NC 27710.
Present address: Department of Biochemistry, University of Illinois at Urbana-Champaign, Urbana, IL 61801.

[1] Abbreviations: CaM, $(Ca^{2+})_4$-calmodulin; COSY, *J*-correlated spectroscopy; DQF, double quantum filter; ECEPP, emperical conformational energy program for peptides; HMQC, heteronuclear multiple quantum correlation; MCD, main-chain directed; NOE, nuclear Overhauser effect; NMR, nuclear magnetic resonance, NOESY, NOE-correlated spectroscopy; rmsd, root mean square deviation; skMLCKp and smMLCKp, skeletal and smooth muscle myosin light-chain kinase calmodulin-binding domain peptides as defined by Seeholzer and Wand (1989) and in the text, respectively; TOCSY, total correlation spectroscopy.

0006-2960/91/0430-10078$02.50/0

modulin-binding domains of the skeletal (Seeholzer & Wand, 1989; Ikura et al., 1991) and smooth (Roth et al., 1991) muscle myosin light-chain kinases (MLCK). In contrast to the growing body of information on the structure of calmodulin in complex with peptide, the structure of a bound peptide has never been determined.

Here we present a multidimensional and multinuclear NMR study of the structure of the smooth muscle myosin light-chain kinase calmodulin-binding peptide bound to calmodulin. The backbound structure of the peptide has been determined to sufficient precision to quantitatively confirm the general features of the helical model for the binding of the MLCK peptides to calmodulin. However, certain local features of the structure indicate that significant distortion of the central helix of calmodulin must occur in order for the bound peptide to satisfy the interactions predicted to occur (by analogy) to the model proposed for the highly homologous skeletal MLCK calmodulin-binding domain peptide (Persechini & Krestinger, 1988).

Materials and Methods

Preparation of Calmodulin and Peptides. Calmodulin was isolated and purified from bovine testicles by hydrophobic interaction chromatography (Gopalarishna & Anderson, 1982) as described previously (Seeholzer & Wand, 1989). Uniformly ^{15}N-labeled calmodulin was prepared as described elsewhere (Roth et al., 1991). The peptide (smMLCKp) used in these studies is based upon the primary sequence of the chicken smooth muscle myosin light-chain kinase calmodulin-binding domain (Kemp et al., 1987). The sequence of peptide smMLCKp is acetyl-A-R-R-K-W-Q-K-T-G-H-A-V-R-A-I-G-R-L-S-NH_2. The unlabeled smMLCKp peptide was prepared by solid-phase peptide synthesis on an Applied Biosystems automatic peptide synthesizer as described previously for the analogous skeletal muscle peptide (Seeholzer & Wand, 1989). ^{15}N-Labeled peptide was synthesized with [α-^{15}N]-tBOC-amino acids using a double coupling strategy and HOBT ester chemistry. Labeled tBOC-amino acid (Merck, 1.5 equiv) was applied during the first coupling. The efficiency of coupling was generally greater than 97% as judged by determination of free amine by ninhydrin. To reduce the creation of deletion peptides, a second cycle of coupling, using unlabeled tBOC-amino acid, was done. Due to the inordinate expense of some [α-^{15}N]tBOC-amino acids, the peptide was labeled only with [α-^{15}N]lysine, -leucine, -valine, -alanine, and -glycine. Both labeled and unlabeled peptides were purified as described previously for the skeletal MLCK calmodulin-binding domain peptide (Seeholzer & Wand, 1989). NMR samples of calmodulin–peptide complexes were prepared from stock solutions of CaM and smMLCKp as described previously (Seeholzer & Wand, 1989) except that ultrafiltration rather than lyophilization was employed. All samples were between 1 and 2 mM of the complex in 10 mM deuterated imidazole and 40 mM Ca^{2+} at pH 6.5 (uncorrected for the isotope effect).

NMR Spectroscopy. All NMR spectra shown were obtained on a Bruker AM600 NMR spectrometer at 25 °C. Standard pulse sequences were used to obtain phase-sensitive DQF-COSY (Rance et al., 1983), spin-locked TOCSY (Bax & Davis, 1985), and NOESY spectra (Macura & Ernst, 1981). Half X-filtered NOESY spectra (Otting et al., 1986) were obtained essentially as described by Fesik et al. (1987). ^1H–^1H correlation and ^{15}N-edited ^1H–^1H correlation spectra were generally derived from data sets composed of 700–800 free induction decays (FIDs) of 1024 complex points. ^{15}N–^1H heteronuclear multiple quantum correlation (HMQC), HMQC-J, and HMQC-NOESY spectra were obtained using pulse sequences described by others (Bax et al., 1983; Kay & Bax, 1990; Gronenborn et al., 1989). A delay of 4.5 ms was used to create ^{15}N–^1H coherence in all experiments. ^{15}N–^1H correlation spectra were generally derived from data sets composed of 400–600 FIDs of 1024 complex points. Three-dimensional NOESY-HMQC spectra were obtained essentially as described by Kay et al. (1989) except that a simple inversion pulse was used to remove ^{15}N precession and J-coupling during the incremented ^1H time domain. All experiments employed direct on-resonance decoupling of the H_2O solvent line. A 128 (^1H) by 120 (^{15}N) by 512 (^1H acquisition) complex point data set was acquired. Each free induction decay was the average of 24 scans. Spectral widths of 7352 Hz for ^1H and 2294 Hz for ^{15}N were used. The spectra were not folded. Time-proportional phase incrementation was used in all experiments to provide quadrature detection during the incremented time domain (Marion & Wüthrich, 1983). Two dimensional spectra were processed to 2K × 2K real points using the FTNMR and FELIX software from Hare Research (Woodinville, WA). Three-dimensional spectra were processed to 512 × 128 × 512 real points with the upfield half of the acquisition frequency domain being discarded. Linear prediction of the first time point was used as required. All spectra shown are referenced to external 3-(trimethylsilyl)-propionate-*2,2,3,3-d*$_4$ at 0.0 ppm for ^1H chemical shifts and to external $(^{15}NH_4)_2SO_4$ at 24.93 ppm for ^{15}N chemical shifts.

Structure Determination. All structure determination calculations were done using the distance geometry computer program Dspace 3.55 and 4.20 (Hare Research, Woodinville, WA). ECEPP geometry was used as templates for amino acid residues (Némethy et al., 1983). Through-space distance constraints were derived from normal, ^{15}N-edited ^1H–^1H NOESY, and ^1H–^1H NOESY-HMQC spectra obtained with a 50-ms mixing time. Lower and upper values for the calibration constant required to convert NOEs to distance ranges were based upon rigid covalent structure (e.g., geminal pairs), global consistency (i.e., minimum violation of covalent geometry) and calibration against NH_i–$C_\alpha H_i$ distances calculated from backbone ϕ angles derived from coupling constants. These intraresidue amide–α coupling constants were estimated by analysis of passive splitting observed in ^{15}N–^1H HMQC-J spectra essentially as described by Forman-Kay et al. (1990) except that a range of values for the double quantum line width (8–12 Hz) was used to allow for variable degrees of internal dynamics. Estimates for the dihedral angle ϕ were obtained using the Karplus equation (Karplus, 1959) and the calibration constants of Pardi et al. (1984). The pattern and relative intensity of the observed backbone NOEs (see Results) for those coupling constants determined to be less than 5 Hz led us to consider only those solutions of the Karplus equation corresponding to negative dihedral angles. The resulting constraints on ϕ were encoded as the distances between N, C, C_α, and O atoms defining the dihedral angle. Prochiral assignments of methylene hydrogens were obtained by the "floating prochiral center" method of Weber et al. (1988). A two-tailed test was used and the assignment of a particular resonance to a specific prochirality used a statistical preference of $p < 0.04$. Generally, refinements of initially embedded structures proceeded in three stages. The first stage consisted of steepest descent nonlinear least-squares minimization with covalent and experimental distance constraints having equal weight. Chirality was corrected, as required, at this stage. The second stage of the refinement involved repetitive cycles of simulated annealing (Nerdal et al., 1988) with covalent and

experimental distance constraints again having equal weight. Structures giving a sum of the squares of violations greater than 1.75 Å^2 were rejected. Approximately one-quarter of embedded structures could be refined to below this threshold. To allow for hydrogen-bond formation, as driven by the inherent covalent and experimental constraints, the effective van der Waals radii of potential H-bond acceptors and donors were reduced to 0.5 of their ECEPP values during all calculations. The structures were then examined for orientation of backbone amide NH and O suitable for hydrogen bonding. Hydrogen bonds were added to the constraint list if the amide NH–carbonyl oxygen distance was less than 2.5 Å in at least 80% of the structures. The final stage of the refinement involved the application of repetitive cycles of simulated annealing during which the covalent geometry of the peptide was constrained using an implementation of the SHAKE algorithm of Rycaert at al. (1977).

RESULTS

The general features of the interaction of smMLCKp with CaM were determined by one-dimensional ^{1}H NMR spectroscopy. Titration of CaM with substoichiometric amounts of smMLCKp results in an ^{1}H NMR spectrum composed of two distinct sets of resonances. One set is derived from free CaM while the second set corresponds to the spectrum of the 1:1 complex between CaM and smMLCKp. This indicates that the interchange of free and bound peptide is in slow exchange on the chemical shift time scale. No additional changes in CaM resonances are observed upon addition of more than 1 equiv of smMLCKp. These results are similar to those obtained during the titration of CaM with peptides corresponding to the CaM-binding domain of skeletal myosin light-chain kinase (Klevit et al., 1985; Seeholzer & Wand, 1989).

Assignment of ^{1}H and ^{15}N Resonances of the Bound Peptide. The ^{1}H resonances arising from smMLCKp bound to CaM were identified by a variety of strategies. As a whole, the CaM–smMLCKp complex (167 amino acid residues) displays a two-dimensional ^{1}H–^{1}H NMR spectrum of considerable complexity [e.g., Figures 3 and 4 in Seeholzer and Wand (1989)]. In an effort to make the assignment of the ^{1}H resonances of the bound peptide straightforward, complexes with α-^{15}N-labeled peptide were used in conjunction with ^{15}N-edited ^{1}H–^{1}H and ^{1}H–^{15}N correlation spectroscopy. An expansion of the amide–amide region of the half X-filtered NOESY spectrum of the 1:1 complex between CaM and ^{15}N-labeled smMLCKp is shown in Figure 1. This spectrum, obtained with a 100-ms mixing time, reveals the ^{1}H–^{1}H chemical shift correlations which are due to the transfer of intensity, via the NOE, from any proton to those amide protons bonded to ^{15}N. All other chemical shift correlations, present in the unedited NOESY, are suppressed. Nine residues of the smMLCKp peptide were α-^{15}N-labeled. Accordingly, the ^{15}N-edited NOESY spectrum is relatively simple. There are, however, several degeneracies of the peptide's amide NH resonances. Sequential amide–amide NOEs are seen throughout the length of the peptide (Figure 1), as are sequential $C_\beta H_i$–NH_{i+1} NOEs (summarized in Figure 4). Amide–amide cross peaks involving Val-12 of the peptide are relatively weak in this spectrum. Most ambiguities present in the ^{15}N-edited ^{1}H–^{1}H NOESY spectrum could be resolved by appealing to ^{15}N–^{1}H HMQC-NOESY spectra (not shown) or to the 3D NOESY-HMQC spectrum. The required assignments of the ^{15}N resonances of the bound peptide were obtained by reference to the ^{15}N-correlated HMQC spectrum shown in Figure 2. This cross assignment was unequivocal.

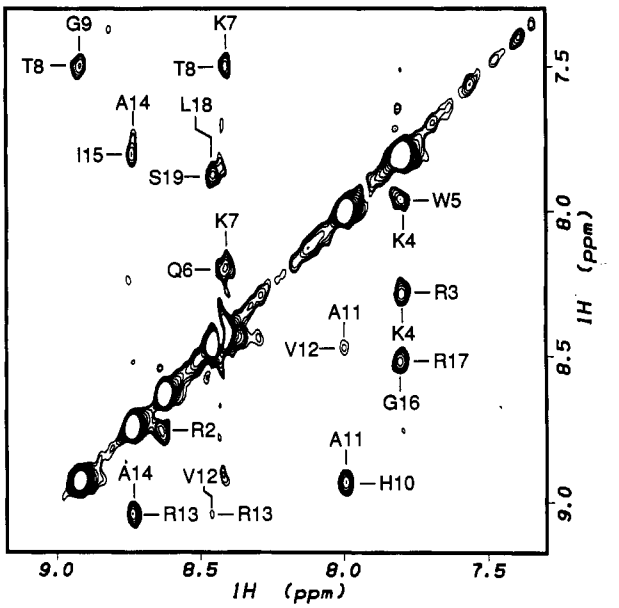

FIGURE 1: Expansion of the half X-filtered NOESY spectrum of the 1:1 bovine CaM–[^{15}N]smMLCKp complex in 90% H_2O/10% H_2O buffer. The mixing time used was 100 ms. Shown are the NOE connectivities of sequential amide protons of the bound peptide. Note that the cross peaks associated with Val-12 of the peptide are relatively weak, as discussed in the text. The sequential residues Gly 9 and His 10, Ile 15, and Gly 16, and Arg 17 and Leu 18 have (nearly) degenerate amide proton chemical shifts, rendering NOEs between these pairs unobservable in this experiment. The NOE correlations between the amide protons of Arg 2 and Arg 3 and between Trp 5 and Gln 6, being unlabeled, do not survive the half X-filter. These correlations are seen in the conventional ^{1}H–^{1}H NOESY spectrum.

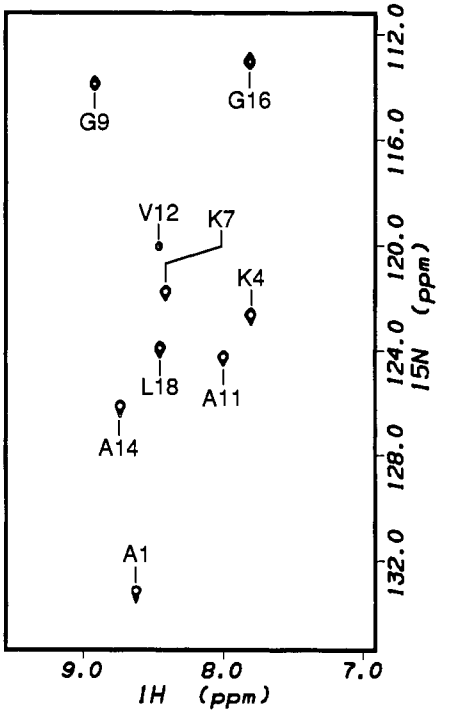

FIGURE 2: Expansion of the HMQC spectrum of the 1:1 bovine CaM–[^{15}N]smMLCKp complex in 90% H_2O/10% D_2O buffer. Indicated are the ^{15}N–^{1}H assignments of the labeled amide nitrogens of the bound peptide.

In the case of the 3D NOESY-HMQC, examination of the ^{1}H vector along the ^{15}N–^{1}H coordinate of each labeled site of the bound peptide was particularly useful in confirming the correctness of the sequence-specific assignments of the main-chain resonances. Examples are shown in Figure 3.

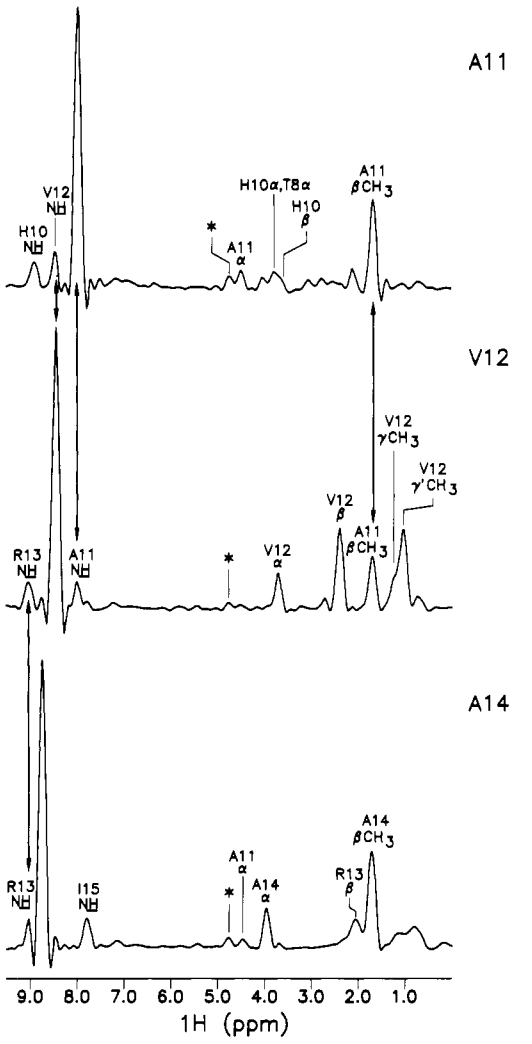

FIGURE 3: Selected vectors from the three-dimensional NOESY-HMQC spectrum of the 1:1 *E. coli* expressed [^{15}N]CaM-[^{15}N]-smMLCKp complex in 90% H_2O/10% D_2O buffer. The mixing time used was 50 ms. Each vector is along the ^{1}H chemical shift dimension at the (^{1}H,^{15}N) coordinate of each labeled site on the peptide. There are no degeneracies between the (^{1}H,^{15}N) resonance pairs of calmodulin and the labeled sites of the bound peptide. The vectors illustrate the clarification of helical MCD NOE patterns by this three-dimensional experiment, for example, by resolving the long-range (i, i + 3) interaction required to overcome the degeneracy of the amide protons of Ile 15 and Gly 16. The asterisks indicate artifacts due to the solvent peak.

Note that, at the mixing time used (50 ms), the intensities of the NOEs arising from Val-12 of the peptide are relatively more intense than those observed in half X-filtered NOESY (Figure 1). Following a strategy outlined previously (Englander & Wand, 1987; Di Stefano & Wand, 1987; Wand & Nelson, 1991), the main-chain NH–C_αH–C_βH ^{1}H subspin systems were defined in ^{1}H–^{1}H DQF-COSY, TOCSY, and NOESY spectra using standard arguments. These provided the primary database required for the assignment of the main-chain resonances of the bound peptide using the main-chain-directed assignment strategy (Englander & Wand, 1987; Wand & Nelson, 1991). Upon completion of the sequence-specific assignment of the backbone amide, α, and β resonances of the bound peptide, many of the side-chain ^{1}H spin systems could be defined in DQF-COSY and TOCSY (35-ms mixing time) spectra using standard arguments. The chemical shifts of assigned resonances are listed in Table I. The chemical shifts of the assigned resonances of the peptide in complex with bovine CaM are indistinguishable from those seen in the *Escherichia coli* expressed chicken CaM–peptide complex. The two calmodulins have identical primary sequences and differ only by the trimethylation of lysine-115 and the N-terminal acetylation of the bovine protein. A summary of the main chain NOEs observed in the bound peptide is presented in Figure 4.

Table I: Resonance Assignments of smMLCKp Bound to Calmodulin

	chemical shift (ppm)[a]				
residue	^{15}N	NH	C_αH	C_βH	other ^{1}H
Ala-1*	133.1	8.63	4.00	1.43	
Arg-2		8.75	4.18	1.30	
Arg-3		8.28	4.06	1.84 (s)	
Lys-4*	122.6	7.79	4.01	1.94	1.72 (γ) 1.54 (δ), 3.20 (ϵ)
Trp-5		7.94	4.17	1.91 (r)	7.24 (2), 7.76 (4), 7.19 (5), 7.24 (6), 7.53 (7)
Gln-6		8.19	3.77	2.06	2.25 (γ)
Lys-7*	121.9	8.41	4.05	2.08	1.90 (γ)
Thr-8		7.48	3.80	4.31	1.05 (γm)
Gly-9*	114.0	8.92	4.14 (r), 3.87 (s)		
His-10		8.93	3.81	3.66 (r)	
Ala-11*	124.3	7.99	4.51	1.69	
Val-12*	120.2	8.47	3.71	2.45	1.17 (r), 1.03 (s)
Arg-13		9.04	4.39	2.12 (r)	
Ala-14*	126.2	8.72	3.96	1.70	
Ile-15		7.78	3.66	2.24	
Gly-16*	113.1	7.79	4.11 (r), 3.87 (s)		
Arg-17		8.52	4.10	2.31	
Leu-18*	124.0	8.48	4.09	1.93 (r)	1.95 (γ), 0.82 (δ), 0.36 (δ)
Ser-19		7.83	4.44	3.88 (r)	

[a] ^{1}H Chemical shifts referenced to external 3-(trimethylsilyl)-propionate-*2,2,3,3-d*$_4$ (coaxial capillary) at 0.0 ppm. ^{15}N Chemical shifts are referenced to external $^{15}NH_4Cl$ at 24.93 ppm. An asterisk indicates ^{15}N-labeled.

Structural Constraints. Though the use of ^{15}N-labeled smMLCKp in conjunction with ^{15}N-edited and ^{15}N-correlated spectroscopy allows the unequivocal assignment of the majority of resonances of the bound peptide, the quantitative interpretation of the intensity of NOEs arising from short-distance interactions between hydrogens of the peptide is problematic. This is because of the possibility that a given NOE cross peak can potentially be due to more than one pair of spins which have degenerate chemical shifts. In this respect, however, the amide NH–C_αH–C_βH subspin systems of the complex have been defined (Roth et al., 1991). This allowed the uniqueness of many of the NOEs observed to be adequately tested. Accordingly, 130 of the 136 NOEs used are between main-chain hydrogens. Quantitative values for involved NOEs were obtained from a standard ^{1}H–^{1}H NOESY spectrum (50-ms mixing time) obtained using a complex prepared with bovine

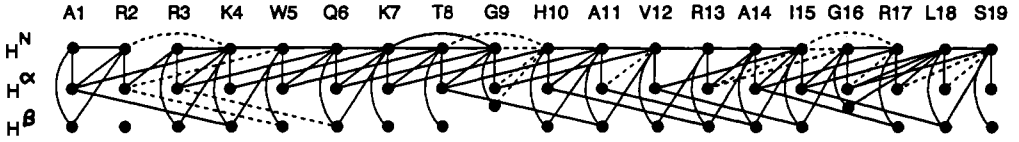

FIGURE 4: Schematic summary of the NOE connectivities observed between main-chain amide, α, and β protons of the smMLCKp peptide bound to calmodulin. Dashed lines indicate the presence of a degeneracy of one or both of the involved protons with resonances of calmodulin or the peptide. The absence of a connectivity corresponds to the absence of NOE intensity.

CaM and unlabeled peptide. All NOEs obtained in this way were compared to those appearing in the various spectra described above. The resulting bounds used in subsequent determination were *widened* as required to be consistent with all data sets. In some cases, where degeneracy was apparent, the NOE intensity was used as a lower bound (23 constraints). In the case of the demonstrable absence of a cross peak, a lower bound of 4.2 Å was imposed (5 constraints).

Additional primary experimental constraints were derived from analysis of passive ^1H–^1H splitting of ^{15}N–^1H cross peaks in HMQC-J spectra of the complex (not shown). Only one labeled residue of the bound peptide, Val-12, shows a resolved splitting (ca. 6 Hz). The remaining eight ^{15}N-labeled residues of the peptide, on the basis of an assumed ^{15}N–^1H double quantum line width of between 8 and 12 Hz, are assigned an NH_i–$C_\alpha H_i$ coupling constant of between 3.5 and 5.5 Hz. These were subsequently encoded in the constraint list as distance constraints corresponding to dihedral ranges of −49° to −87° and −113° to −127° for unresolved splittings (<5 Hz) and the one resolved splitting, respectively.

Summary of the Refinement. The refinement of the structure of the bound peptide proceeded in three stages. The first stage allowed all prochiral centers to "float". Structures were embedded and refined by sequential application of steepest descent minimization of the summed squares of violations and simulated annealing with covalent and experimental constraints equally weighted. Sixty-four structures having a final sum of the squares of the violations of less than 2.5 Å^2 were then pooled and used to examine potential main-chain hydrogen bonding. This family of structures had no chiral violations and no violations greater than 0.4 Å. Sixty-four additional structures were generated with constraints having prochiral labeling opposite to that used above. This family of structures has similar refinement characteristics. Standard (i, i + 4) α-helical hydrogen bonding was observed from residue 4 through 11 (acceptors) and from residue 13 to 14 (acceptors) in at least 80% of the structures on the basis of the requirement that the donor NH and acceptor CO be within 2.5 Å of each other. The carbonyl of Val-12 did not show any intrapeptide hydrogen-bonding orientations. The determined hydrogen bonds were encoded in the constraint list for subsequent refinements. Specific prochiral assignments of several methylene hydrogens could also be determined for eight prochiral centers using the floating chirality method (Weber et al., 1988). These were encoded in the constraint list used in subsequent refinements and are noted in Table I. The second stage of the refinement involved the application of simulated annealing to the 128 structures using the additional hydrogen-bonding constraints [CO(i) to NH(i + 4) distance of 1.8–2.1 Å] and prochiral assignments determined above. The 64 structures having the lowest summed squares penalty were then pooled. This family of structures had no chiral violations and an average sum of the squares of all violations of 1.3 Å. All structures were subsequently refined to a sum of the squares of the violations of less than 0.6 Å^2 by repetitive application of simulated annealing during which the covalent geometry of the peptide was constrained using an implementation of the SHAKE algorithm (Rycaert et al., 1977). This family of structures had no chiral violations, an average sum of the squared violations of 0.49 Å^2, and no violations greater than 0.2 Å. Superpositions of the main-chain N, C_α, and C atoms of all residues results in an average rmsd from the mean structure of 0.90 Å. Most of the variation between structures lies in the first three and last residues of the peptide. Superpositions of the main-chain atoms of residues 4–18 results in an average rmsd from the mean structure of 0.44 Å. The distribution of violations among the various types of constraints used are summarized in Table II.

Table II: Summary of Average Violations of the Structure of smMLCKp Bound to Calmodulin

	average violation (Å)[a]	
constraint type	lower bound	upper bound
bond	1.327 (0.183)	1.786 (0.239)
angle[b]	1.216 (0.166)	1.434 (0.190)
rigid[c]	0.466 (0.107)	0.646 (0.108)
VDW	1.141 (0.253)	*d*
experimental	1.961 (0.235)	0.887 (0.267)
hydrogen bond	0.093 (0.055)	0.168 (0.065)
triangle[e]	*d*	0.184 (0.130)
$\sum$ violations	11.309 (1.503)	
$\sum$ (violations)^2 (Å^2)[f]	0.494 (0.165)	

[a] Given is the average, per structure, of the sum of the violations of each class of constraint considering all atoms. The standard deviation about each mean is listed in parentheses. [b] Average of the sum of the violations of the fixed distances between geminal atoms defining rigid angles. [c] Average of the sum of the violations of distance constraints used by Dspace to enforce planarity and other rigid-body features of the covalent structure. [d] Not applicable. [e] Average of the sum of the violations of distance constraints derived from application of the triangle inequality. [f] Note, the distribution is asymmetric and is skewed to smaller values.

Table III: Backbone Conformation of smMLCKp Bound to Calmodulin

	average dihedral angle (deg)[a]	
residue	ϕ	ψ
Ala-1	*b*	−44.6 (65.7)
Arg-2	−6.0 (68.6)	−45.4 (94.6)
Arg-3	−38.2 (88.9)	−9.3 (50.3)
Lys-4	−62.0 (5.7)	−46.8 (15.3)
Trp-5	−72.9 (6.8)	−35.3 (14.6)
Gln-6	−62.8 (4.5)	−38.1 (6.6)
Lys-7	−61.9 (2.1)	−50.0 (9.8)
Thr-8	−72.3 (6.8)	−25.5 (16.8)
Gly-9	−69.3 (9.8)	−35.1 (7.6)
His-10	−64.0 (5.4)	−34.9 (7.2)
Ala-11	−59.8 (2.5)	−62.9 (6.9)
Val-12	−67.2 (3.5)	−44.9 (14.3)
Arg-13	−59.3 (3.4)	−49.5 (20.1)
Ala-14	−57.7 (9.8)	−44.2 (14.8)
Ile-15	−60.7 (2.9)	−43.7 (18.9)
Gly-16	−79.6 (1.7)	−21.6 (18.5)
Arg-17	−64.2 (8.8)	−26.4 (7.7)
Leu-18	−68.8 (2.5)	−49.2 (9.9)
Ser-19	−89.5 (59.5)	*b*

[a] Standard deviation in parentheses. [b] Not constrained.

Structure of smMLCKp Bound to CaM. The pattern of NOEs observed to occur between main-chain amide NH, $C_\alpha H$, and $C_\beta H$ protons of the smMLCKp peptide bound to the calcium-saturated state of calmodulin (Figure 4) is generally indicative of an α-helical conformation (Wüthrich et al., 1984; Wand & Nelson, 1991). The quantitative evaluation of the NOEs and J coupling constraints results in a structural model which reflects not only the general helical character of the pattern of main-chain NOEs but also various local exceptions to it. The main chain of the structural model is well constrained throughout the majority of the peptide (Table III). The ϕ and ψ dihedral angles associated with residues 1, 2, 3, and 19 of the peptide are relatively poorly defined. In contrast, the backbone dihedral angles defining the conformation of residues 5–18 are very well determined. It should be noted that the ϕ angle determined for Val-12 violates the primary constraints on this angle (encoded as distances with equal weight with all other primary constraints). The violations are small, generally less than 0.1 Å. With three exceptions, the

mean ϕ and/or ψ angles associated with each residue are within 2.5 standard deviations of those corresponding to the average angles observed in high-resolution structures of proteins [−62° and −41°, respectively (Barlow & Thornton, 1988)]. The ϕ angles associated with residues Gly-16 and Leu-18 and the ψ angle associated with Ala-11 have mean values significantly different than the average values for an α-helix (Table III). There are several instances where longer range (i, i + 3) NOEs, expected for a uniform α helix, are absent. For example, the backbone ϕ angles from residue 5–10 of the bound peptide, though close to the expected values for an α helix, are uniformly more negative. This correlates well with the absence of ($C_\alpha H_i$, $C_\beta H_{i+3}$) NOEs throughout this region of the peptide. Although poorly determined, the mean ϕ and ψ angles for residues 2 and 3 are more consistent with a turn rather than a standard α-helical conformation. Finally, though a number of NOEs between the side chains of the peptide and the backbone were used in the above calculations, they are insufficient to constrain the side chains with reliable precision (average rmsd of 1.7 Å for all atoms of residues 4–18 to the mean structure).

Discussion

A central issue in developing an understanding of the structural parameters which govern the calmodulin-mediated regulation of numerous enzymes is whether or not the calmodulin-binding domains of these proteins form a common structural motif in complex with calcium-saturated calmodulin. Studies with peptides based upon naturally occurring sequences, some corresponding to the calmodulin-binding domain of target enzymes [e.g., Blumenthal et al., (1985), Kemp et al. (1987), Dasgupta et al. (1989), and Vorherr et al. (1990)] and some not [e.g., McDowell et al. (1985) and Comte et al. (1983)], have indicated a general basic amphiphilic sequence requirement. The common interpretation of these studies has been the conclusion that calmodulin-binding peptides form a regular α-helical structure upon association with calmodulin. The amphiphilic helix model, in the context of physiologically relevant peptides, has rested on indirect evidence such as data obtained from difference circular dichroism (Klevit et al., 1985) and is buttressed by the general correspondence of the ^{1}H spectrum of melittin in methanol to the spectrum of melittin in the 1:1 complex with perdeuterated CaM (Seeholzer et al., 1987). The most striking and direct evidence for the formation of α-helical secondary structure by peptides in high-affinity complexation with calmodulin has come from the model peptide experiments of DeGrado and co-workers [e.g., Cox et al. (1985), O'Neil et al. (1987), and O'Neil and DeGrado (1990)]. These studies culminated in the report that the fluorescence properties of a tryptophanyl residue systematically moved throughout the sequence of an amphiphilic model peptide display a periodicity very close to that expected for a helical conformation (O'Neil et al., 1987). However, it was also pointed out that the profiles of the three fluorescence parameters used to investigate the periodicity of interaction of peptides with calmodulin deviated significantly from the strict periodicity examined. Several explanations were discussed, some recognizing the possible positional dependence upon the interaction of calmodulin with the fluorescence probe and some recognizing the possibility of (small) local deviations of the peptide's structure away from a strictly α-helical conformation. Both classes of explanations in turn raise the question of the effects of sequence heterogeneity of the various physiologically relevant peptides upon their local structure while bound to calmodulin. Nonetheless, since that classic study, the basic assumption that physiologically relevant peptides strictly conform to the amphiphilic helix model has often been used in model-building efforts aimed at developing working models for the structure of calmodulin–peptide complexes [e.g., Persechini and Kretsinger (1988)]. The studies presented here help resolve some of the potential issues related to this assumption.

The general features of the backbone conformation of smMLCKp peptide bound to calcium-saturated calmodulin conform to the expectations of the amphiphilic helix model. The three exceptions to α-helical conformation, noted above, are interesting in two respects. On the one hand, the nonhelical backbone dihedral angles found at positions 11 and 16 correspond closely to the analogous positions (residues 10 and 14, respectively) in the model peptides where significant deviation from the strict periodicity of fluorescence properties was observed (O'Neil et al., 1987). Thus, the structure of the bound smMLCKp peptide, if analogous to the model peptides, explains the behavior of the latter. More important, the deviation of the backbone from that of a strict α-helix points to the possibility that the working model developed for the complex between calmodulin and the homologous skeletal MLCK calmodulin-binding domain peptide (Persechini & Krestinger, 1988) may not be entirely applicable to the interactions of smMLCKp with calmodulin. The deviations from an α-helical conformation in the peptide require that significantly more distortion of the central helix of calmodulin be introduced in order for the integrity of the globular domains of calmodulin to be maintained while, at the same time, satisfying the analogous (predicted) contacts between smMLCKp and CaM (Roth et al., unpublished results). Indeed, it has been demonstrated that the backbone conformations of the globular domains of calmodulin do not change noticeably upon association with either the skMLCKp (Seeholzer & Wand, 1989; Ikura et al., 1991) or smMLCKp (Roth et al., 1991) peptides while the middle residues of the central helix, in both complexes, appear to adopt an extended chain conformation.

With the backbone conformation of the smMLCKp peptides as well as extensive resonance assignments of calmodulin (Roth et al., 1991) and of the peptide (Table I) now in hand, we can undertake the comprehensive search required to delineate the NOE contacts between the peptide and calmodulin with the ultimate goal of generating a detailed structural model for the complex.

Acknowledgments

We thank Dr. R. A. Beckman for modification of Dspace templates and for discussion of the determination of prochiral assignments by statistical methods. We are also grateful to Dr. D. Hansburg and S. Nakajima for preparation of the smMLCKp peptides.

Supplementary Material Available

One table listing the NOE-based distance constraints used to generate the structure of the smMLCKp peptide bound to calcium-saturated calmodulin (2 pages). Ordering information is given on any current masthead page.

References

Alexander, K. A., Watkim, B. T., Doyle, G. S., Walsh, K. A., & Storm, D. R. (1988) *J. Biol. Chem. 263*, 7544–7549.

Babu, Y. S., Sack, J. S., Grennhough, T. J., Bugg, C. E., Means, A. R., & Cook, W. J. (1985) *Nature 315*, 37–40.

Babu, Y. S., Bugg, C. E., & Cook, W. J. (1988) *J. Mol. Biol. 204*, 191–204.

Barlow, D. J., & Thornton, J. M. (1988) *J. Mol. Biol. 201*, 601–619.

Bax, A., & Davis, D. G. (1985) *J. Magn. Reson. 65*, 355–360.
Bax, A., Griffey, R. H., & Hawkins, B. L. (1983) *J. Magn. Reson. 55*, 301–315.
Blumenthal, D. K., Takio, K., Edelman, A. M., Charbonneau, H., Titani, K., Walsh, K. A., & Krebs, E. G. (1985) *Proc. Natl. Acad. Sci. U.S.A. 82*, 3187–3191.
Comte, M., Maulet, Y., & Cox, J. A. (1983) *Biochem. J. 209*, 269–272.
Cox, J. A., Comte, M., Fitton, J. E., & DeGrado, W. F. (1986) *J. Biol. Chem. 260*, 2527–2534.
Dasgupta, M., Honeycutt, T., & Blumenthal, D. K. (1990) *J. Biol. Chem. 264*, 17156–17163.
Di Stefano, D. L., & Wand, A. J. (1987) *Biochemistry 26*, 7272–7281.
Englander, S. W., & Wand, A. J. (1987) *Biochemistry 26*, 5953–5958.
Fesik, S. W., Gampe, R. T., Jr., & Rockway, T. W. (1987) *J. Magn. Reson. 74*, 366–371.
Forman-Kay, J. D., Gronenborn, A. M., Kay, L. E., Wingfield, P. T., & Clore, G. M. (1990) *Biochemistry 29*, 1566–1572.
Gopalakrishna, R., & Anderson, W. B. (1982) *Biochem. Biophys. Res. Commun. 104*, 830–836.
Gronenborn, A. M., Bax, A., Wingfield, P. T., & Clore, G. M. (1989) *FEBS Lett. 243*, 93–98.
Ikura, M., Kay, L. E., & Bax, A. (1990) *Biochemistry 29*, 4659–4667.
Ikura, M., Kay, L. E., Krinks, M., & Bax, A. (1991) *Biochemistry 30*, 5498–5504.
Karplus, M. (1959) *J. Phys. Chem. 30*, 11–15.
Kay, L. E., & Bax, A. (1990) *J. Magn. Reson. 86*, 110–126.
Kay, L. E., Marion, D., & Bax, A. (1989) *J. Magn. Reson. 84*, 72–84.
Kemp, B. E., Pearson, R. B., Guerriero, V., Jr., Bagchi, I. C., & Means, A. R. (1987) *J. Biol. Chem. 262*, 2542–2548.
Klevit, R. E., Blumenthal, D. K., Wemmer, D. E., & Krebs, E. G. (1985) *Biochemistry 24*, 8152–8157.
Macura, S., & Ernst, R. R. (1980) *Mol. Phys. 41*, 95–117.
Marion, D., & Wüthrich, K. (1983) *Biochem. Biophys. Res. Commun. 113*, 967–974.
McDowell, L., Sanya, G., & Prendergast, F. G. (1985) *Biochemistry 24*, 2979–2984.
Nemethy, G., Pottle, M. S., & Scheraga, H. A. (1983) *J. Phys. Chem. 87*, 1883–1887.
Nerdal, W., Hare, D. R., & Reid, B. R. (1988) *J. Mol. Biol. 201*, 717–721.
O'Neil, K. T., & DeGrado, W. F. (1985) *Proc. Natl. Acad. Sci. U.S.A. 82*, 4954–4958.
O'Neil, K. T., & DeGrado, W. F. (1990) *Trends Biochem. Sci. 15*, 59–64.
O'Neil, K. T., Wolfe, H. R., Jr., Erickson-Viitanen, S., & DeGrado, W. F. (1987) *Science 236*, 1454–1456.
Otting, G., Senn, H., Wagner, G., & Wüthrich, K. (1986) *J. Magn. Reson. 70*, 500–505.
Pardi, A., Billeter, M., & Wüthrich, K. (1984) *J. Mol. Biol. 180*, 741–751.
Persechini, A., & Kretsinger, R. H. (1988) *J. Cardiovasc. Pharmacol. 12* (Suppl. 5), S1-S12.
Rance, M., Sorensen, O. W., Bodenhausen, G., Wagner, G., Ernst, R. R., & Wüthrich, K. (1983) *Biochem. Biophys. Res. Commun. 117*, 479–485.
Roth, S. M., Schneider, D. M., Strobel, L. A., VanBerkum, M. F. A., Means, A. R., & Wand, A. J. (1991) *Biochemistry* (submitted for publication).
Rycaert, J. P., Ciccotti, G., & Berendsen, H. J. C. (1977) *J. Comp. Phys. 23*, 327.
Seeholzer, S. H., & Wand, A. J. (1989) *Biochemistry 25*, 4011–4020.
Seeholzer, S. H., Cohn, M., Putkey, J., Means, A. R., & Crespi, H. L. (1986) *Proc. Natl. Acad. Sci. U.S.A. 83*, 3634–3638.
Strynadka, N. C. J., & James, M. N. G. (1990) *Proteins: Struct., Funct., Genet. 7*, 234–248.
Vorherr, T., James, P., Krebs, J., Enyedi, A., McCormick, D. J., Penniston, J. T., & Carafoli, E. (1990) *Biochemistry 29*, 355–365.
Wand, A. J., & Nelson, S. J. (1991) *Biophys. J. 59*, 1101–1112.
Weber, P. L., Morrison, R., & Hare, D. R. (1988) *J. Mol. Biol. 204*, 483–487.
Wüthrich, K., Billeter, M., & Braun, W. (1984) *J. Mol. Biol. 180*, 715–740.